#1

University of Missouri – Rolla
School of Mines and Metallurgy

Anode, Cathode and Thin Film Studies for Low Temperature SOFC's

Final Report
Period 11/1/98 - 10/31/99

Reporting Period Start Date:	11/1/98
Reporting Period End Date	10/31/99
Principal Authors	Dr. Wayne Huebner Dr. Harlan U. Anderson
Date Issued:	November 1999
DOE Award Number	DE-FG26-98FT40487
Submitting Organization	University of Missouri - Rolla Ceramic Engineering 222 McNutt Hall 1870 Miner Circle Rolla, MO 65409-0810

Phone: (573) 341-6129
FAX: (573) 341-6934
email: huebner@umr.edu

DISCLAIMER

ABSTRACT

In this research the microstructure ↔ property relations in solid oxide fuel cells (SOFC's) are being studied to better understand the mechanisms involved in cell performance. The overall aim is to fabricate SOFC's with controlled, stable, high performance microstructures. Most cathode studies were completed in the last DOE contract; studies during this year focused more on the influence of nonstoichiometry on the electrical performance. Studies indicate that nonstoichiometric $La_xSr_{0.20}MnO_3$(x=0.70, 0.75, and 0.79) cathode compositions exhibit the best properties. A series of studies using these compositions fired on at temperatures of 1100, 1200, 1300 and 1400°C were performed. In all instances, 1200°C was the optimum, with the x=0.70 composition being the best. It has an overpotential of only 0.04V at 1 A/cm^2. SEM analyses indicated no second phases or interdiffusion is detectable.

Studies on optimization of anode compositions yielded the optimum volume fraction of Ni (45vol%), the best sintering temperature / time (1400°C/2 h), and the best starting materials (glycine-nitrate derived NiO and "normal" YSZ). In essence these results simply reflect the optimum microstructure. As such, they are being used to guide the development of optimized anodes for lower temperature operation based on Cu/CeO_2 cermets.

Marked success has been achieved on the placement of thin YSZ electrolytes on porous Ni/YSZ electrodes. The process being used is a "transfer technique" in which dense YSZ films are initially fabricated on NaCl or polymeric substrates, followed by partial dissolution of the substrate and placement of the film on the porous substrate. This technique has allowed us to produce structures with film thicknesses ranging from 70 to 3000 nm, and grain sizes ranging from 2 to 300 nm. Cells based on electrolytes this thick should operate in the 400 – 700°C range.

Table of Contents

LIST OF FIGURES

1.0 INTRODUCTION

Materials research focused on solid oxide fuel cells (SOFC) is driven by the recognition that processing and operating at lower temperatures would not only directly address many reliability problems, but would also have the potential of leading to lower cost manufacturing and lowering the cost of energy produced from the resulting power plants. Hence numerous research groups around the globe are in pursuit of alternate materials for all four SOFC components. Research has focused on materials with higher conductivities at lower temperatures, mixed-conducting cathodes, novel synthesis techniques (for powders and thin films), controlled and stable microstructures, and chemical, mechanical, and electrical stability under the conditions of co-firing and operation. Over the course of this one year project (DE-FG26-98FT40487) research has focused on: 1) completing a set of studies on the influence of nonstoichiometry of the cathode (LSM-based) on the cell performance, 2) completing sets of studies on the influence of Ni particle size on the anode performance, and 3) developing thin film electrolytes based on simple spin-coating approaches. All three of these tasks were successful, and represent enabling strides forward towards the goal of lower temperature SOFC's.

2.0 EXECUTIVE SUMMARY

Results from studies over this past year can be simply summarized as follows:

Cathode Studies:

- Increasing the particle size of the $La_{1-x}Sr_xMnO_3$ cathode results in higher overpotentials, but lends long term stability at 1000°C. Increasing the cathode firing temperature increases the overpotential, although the microstructure remains fairly constant. Although 800°C yields the best initial results, after 24 h of operation the overpotential climbs sharply. We have found that 1000°C gives the best performance/stability combination. At 1 A/cm^2, the cathodic overpotential is ≈0.1 V, which is very good

- Nonstoichiometric $La_xSr_{0.20}MnO_3$(x=0.70, 0.75, and 0.79) cathode compositions exhibit the best properties. Previously-summarized results showed that A-site deficient compositions exhibited the lowest overpotentials. To further explore this effect, we completed a series of studies using these compositions fired on at temperatures of 1100, 1200, 1300 and 1400°C. In all instances, 1200°C was the optimum, with the x=0.70 composition being the best. It has an overpotential of only 0.04V at 1 A/cm^2. SEM analyses indicated no second phases or interdiffusion is detectable. Longer time studies are underway.

Anode Studies

- YSZ anodes prepared with lower Ni volume fractions (40 & 45%) resulted in lower overpotentials and improved stability.

- Higher sintering temperatures effectively lowered the overpotential and increased the in-plane conductivity. Due to constrained sintering between the anode and the YSZ electrolyte, higher sintering temperatures allowed more densification in the z-direction, resulting in a rigid YSZ structure to support Ni particles

- By decreasing the densification between Ni grains, there are more paths for conduction (more Ni-Ni contacts throughout the structure and higher conductivities) and a larger number of Ni-YSZ contacts (lower overpotentials).

- The 45 vol% Ni composition co-fired with the electrolyte had the lowest initial overpotential of any cermet with a similar composition.

Thin Film Electrolyte Studies

- Marked success has been achieved on the placement of thin YSZ electrolytes on porous Ni/YSZ electrodes. The process being used is a "transfer technique" in which dense YSZ films are initially fabricated on NaCl substrates, followed by partial dissolution of the substrate and placement of the film on the porous substrate. Heating the substrate to 400°C results in a firmly attached films; higher temperatures result in grain growth. This technique has allowed us to produce structures with film thicknesses ranging from 70 to 3000 nm, and grain sizes ranging from 2 to 300 nm. I-V measurements of single cells produced by this technique have been initiated within the last month. However, the early results are very encouraging and indicate that we indeed can produce dense, nonporous YSZ electrolytes at temperatures in the 400 to 700°C range. These results are currently serving as a vehicle in which the influence of microstructure and electrolyte thickness on cell performance can be evaluated.

3.0 EXPERIMENTAL PROCEDURE

3.1 Materials Selection, Preparation and Characterization

The YSZ electrolyte used in the cathode and anode investigations was self supporting (≈200 μm thick). Cathode and anode compositions were applied via screen printing onto a pre-sintered dense electrolyte. A flowchart describing the techniques used to fabricate single cells is shown in the accompanying figure. Commercially available Y-stabilized ZrO_2 (YSZ - Zirconia Sales of America) powders were used in this study for the electrolyte and as a major constituent in the anode. It is a fully stabilized (8 mole % Y_2O_3), co-precipitated powder, with a primary particle size of approximately 250 nm and a corresponding BET surface area of ~ 8.0 m^2/g. NiO, and Mg-doped NiO were synthesized using the glycine nitrate method with $Ni(NO_3)_2 \cdot xH_20$, $MgCO_3$, glycine, and distilled water as the starting materials. Powder crystallinity, phase, and surface area were characterized using X-ray diffraction and BET techniques as a function of calcination temperature. A YSZ-NiO (45 vol % Ni) composition was also prepared in which both components were combusted simultaneously using the glycine nitrate process. Starting raw materials were $Ni(NO_3)_2 \cdot xH_20$, $Y(NO_3)_3 \cdot xH_20$, and a zirconium citrate complex.

A total of three different techniques were used to prepare anode powder mixtures with the goal of producing different resultant microstructures including: 1) mixing YSZ with $Ni_{1-x}Mg_xO$ (x=0.0, 0.1, 0.2), 2) mixing YSZ with NiO followed by calcination at 1400°C for 4 h, and 3) simultaneous combustion of both components using the glycine nitrate technique. Anode powders were mixed with a commercial resin solution, BX018-16, from Ferro Corp. The suspension was mixed using a three roll mill to prepare a well-dispersed paste for screen printing. In all instances the highest amount of powder was loaded into the binder such that the paste was still workable, typically 50 to 75 wt%. Anode compositions were screen printed onto dense YSZ electrolytes and sintered onto the electrolyte between 1300°C and 1500°C in 100°C increments for a 1 h hold, with a heating and cooling rates of 3°C/min. A goal of this investigation was to investigate the influence of grain size and porosity of the electrode on the cell performance, therefore powders were calcined and sintered at various temperatures. Anodes were porous, exhibited grain sizes on the order of 1 μm, and gave resultant dimensions of 0.635 cm x 0.635 cm and ≈ 20 μm thick.

$La_xSr_{0.2}MnO_3$ ($0.7 \leq x \leq 0.79$) compositions were synthesized by the liquid mix technique using $La_2(CO_3)_3$, $SrCO_3$, and $MnCO_3$ as the raw materials. All raw materials were standardized

thermogravimetrically to determine the cation concentration. The carbonates were dissolved in nitric acid, ethylene glycol, citric acid and water in glass beakers. Heating resulted in the formation of a polymeric precursor solution which was then oxidized at ~300°C. The powder was vibratory milled dry for 4 h with ZrO_2 media. The powder was then calcined in MgO crucibles at temperatures of 800 - 1200°C in increments of 100°C. Soak times for all calcinations were 4 h. The powders were vibratory milled again using the same conditions as described before. Powder crystallinity, phase, and surface area were characterized using X-ray diffraction and BET techniques as a function of calcination temperature.

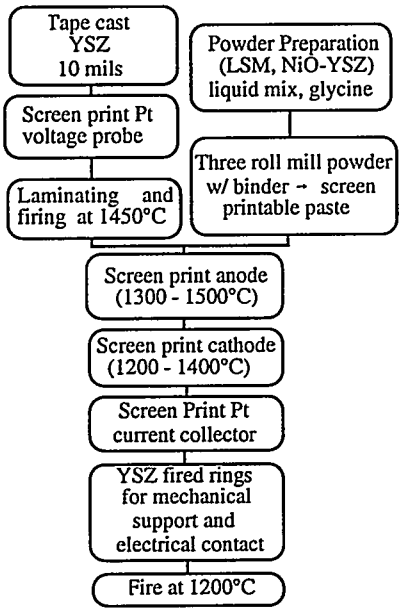

Flowchart of the techniques used for fabricating single cells.

A porous Pt grid (0.2 mm line width and 0.2 mm spacing) was screen printed on the electrodes for cell performance experiments to act as a current collector, and allow gas diffusion to the electrode/electrolyte interface, figure 1. The rings were designed with pads which were coated with Pt paste to allow for electrical sensing. Pt wires of 10 mil diameter were bonded from the Pt grid to the Pt pads on the rings using Pt paste, this was done to both the anode and cathode side of the electrolyte. Pt paste was also used as the connection between the Pt voltage probe and a pad on the ring for voltage sensing. There are 2 pads on the cathode side: one for electrical connection to the cathode and one for sensing the voltage probe. Only one pad was active on the anode side. The cell was sintered at 1200°C for 1 h to densify the Pt and achieve a good bond between the YSZ rings and electrolyte.

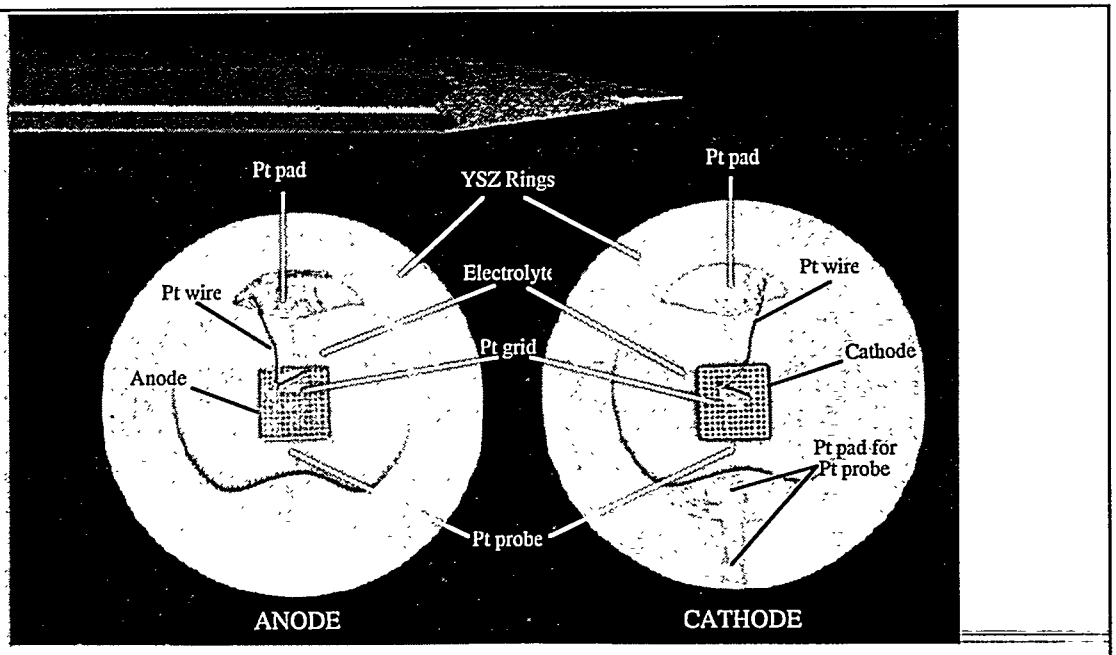

Figure 1. YSZ rings bonded to the electrolyte for mechanical support and electrical contact.

3.2 Electrical Characterization

Electrical characterization of single cells utilizing the internal Pt voltage probe was investigated to simultaneously separate the losses attributed to each component (anode, electrolyte, cathode) and their interfaces (cathode/electrolyte and anode/electrolyte) during cell operation. The cell performance studies were focused on the reaction kinetics at the interfaces whereas DC conductivity measurements were performed to investigate the resistive losses of each component as a function of time, composition, and preparation condition.

Electrochemical (I-V) measurements were carried out using a five electrode configuration, which allowed for separation of anode and cathode overpotentials during operation, figure 3. Separate leads were used to carry the current and voltage of the cell to remove the loss associated with the lead wires and allow for a direct examination of the losses attributed to the cell components. The third voltage lead was connected to the voltage probe and was used to monitor the voltage drop between the probe and corresponding electrodes during operation. Pt wires were used on the cathode side, four 20 mil wires for the current lead, and 10 mil wires for both the voltage leads, cathode and internal Pt probe. Ni wires were used on the anode side, two 20 mil wires for the current lead and a 10 mil wire for the voltage lead. Both voltage leads for the cathode and anode were designed to mimic a spring for contact with the Pt grids.

I-V behavior and AC impedance spectroscopy were performed on both half cells and complete cells. The I-V behavior was measured using an Anatronics Current/Voltage Control Fuel Cell Testing Module, a Keithley Model 196 Microvolt Meter, and a Fluke 27/FM Multimeter. The Fuel Cell Testing Module was placed in the voltage control mode thus enabling the desired cell voltage and corresponding current to be measured. AC impedance measurements were performed with a computer controlled Solartron 1260 Impedance/Gain-Phase Analyzer over the frequency range of 0.01 Hz to 100kHz with an applied signal of 20 mV.

After the cell was heated to 1000°C at ~ 2°C/min, air was first fed to the cathode and then the fuel was introduced to the anode. The fuel was delivered to the anode for at least thirty minutes before electrical contact was made to ensure that the anode (YSZ-NiO) was reduced to the cermet (YSZ-Ni). It could also be determined at this time if the electrolyte was cracked or the sealant had failed. The resistance between the voltage and current leads of each corresponding electrode was measured before testing to ensure that each lead was still connected to the Pt grid and thus the electrode.

After all electrical connections were made the first test was to measure the open circuit, Nernst potential between the anode and cathode. The Nernst potential is very sensitive to the

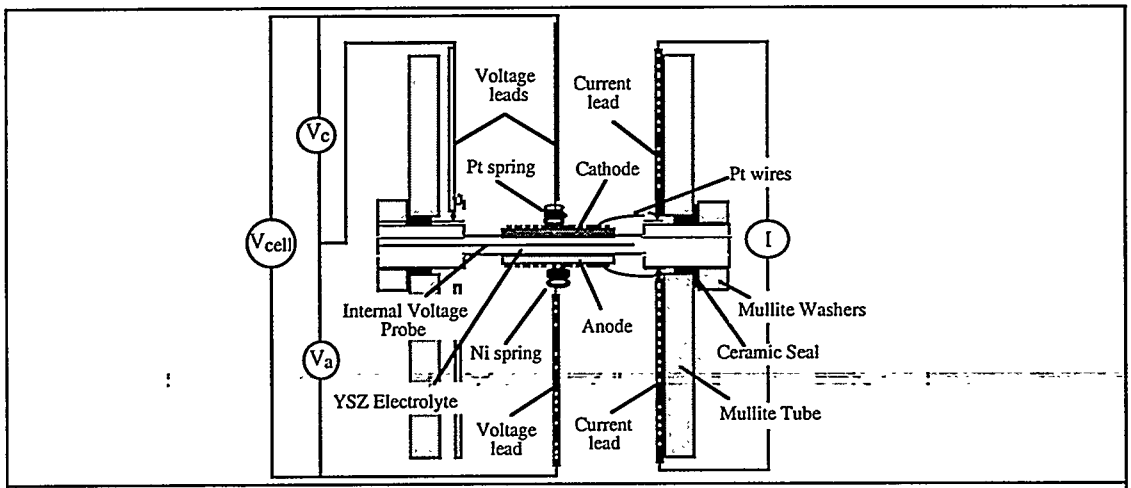

Figure 2. Experimental set up used for measuring the electrochemical (I-V) behavior of single cells.

chemical potential gradient and hence reveals whether a small hairline fracture had occurred. It was often difficult to tell this by monitoring the exit ball flow meters and were thus a better test for fractures or leaks.

Measurements were carried out from small voltages to larger ones in increments of 25mV and in all cases steady state voltages and currents were measured. Stabilization times were on the order of 2-3 min. The current, total cell voltage (V_{cell}), voltage drop from the Pt probe to the cathode (V_c) and the anode (V_a) were all simultaneously measured. At open circuit and at any given voltage under load the total cell voltage was equal to the two half cell voltages.

$$V_{cell}(I) = V_c(I) + V_a(I)$$

Overpotentials were calculated by subtracting the voltage drop under load from the corresponding voltage drop at open circuit:

$$\eta_{anode/cathode}(I) = V_c@O.C. - V_c(I) - IR_{electrolyte} - IR_{anode/cathode} \quad [2]$$

where

$\eta_{anode/cathode}(I)$	=	anodic overpotential
$V_c@O.C.$	=	voltage drop between cathode and Pt probe at open circuit
$V_c(I)$	=	voltage drop between cathode and Pt probe under load
$IR_{electrolyte}$	=	voltage drop associated with the electrolyte (100 μm thick)
$IR_{anode/cathode}$	=	voltage drop associated with the anode

4.0 Results and Discussion

This report is divided into three sections corresponding to studies on anodes, cathodes, and thin film electrolytes.

4.1 Anode Studies

Resistive (IR) Contribution from the Anode

Four point DC conductivity experiments were performed on anode compositions to determine the resistive loss associated with the anode during cell operation. Anode conductivities ranged from ≈3 - 800 S/cm which depended on the starting raw materials, fabrication technique, and the sintering temperature. Figure 3 is a typical V-I plot of an anode demonstrating ohmic behavior. From the dimensions of a screen-printed anode then, for a current density of 1000 mA/cm^2 the voltage drop in the anode would be at most 0.7 mV. Hence the measured voltage as a function of current density between the anode and the Pt voltage probe can be attributed solely to the resistive loss of the electrolyte and the overpotential of the anode.

Effect of Vol % Ni on Anodic Overpotentials

Compositions studied for this experiment ranged from 40-55 vol % Ni in increments of 5 vol %. Oxide powder mixtures were calcined at 900°C, sintered on the YSZ electrolyte at 1400°C, and then reduced in situ. After the fuel was introduced to the anode, the cell was allowed to stabilize for ~ 1-3 h before electrochemical measurements were performed. Conductivity

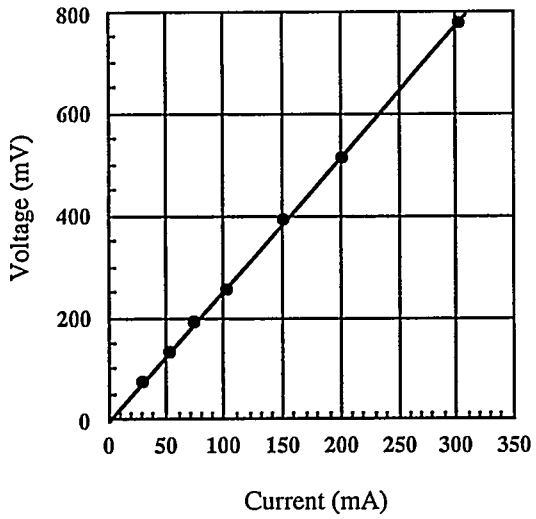

Figure 3. V-I behavior for a Ni-YSZ cermet.

experiments were monitored in air, during reduction of NiO to Ni, and under reducing conditions for 24 h.

The electrochemical response of the four compositions is shown in Figure 4. The 40 and 45 vol% Ni samples show similar behavior, ≈220 mV and 200 mV at 1000 mA/cm^2, but the 50 and 55 vol % compositions showed much higher overpotentials, ≈280 and 370 mV at 1000 mA/cm^2. After 24 h, the overpotentials of all compositions increased, Figure 5. The 40 and 45 vol % Ni samples still show similar behavior, ≈270 mV at 1000 mA/cm^2, and the 50 and 55 vol % Ni compositions had overpotentials of ≈370 and 470 mV at 1000 mA/cm^2. The low vol % Ni samples, 40 and 45, have the lowest overpotentials due to the larger YSZ content in the cermet to support the Ni particles. This would effectively reduce the amount of sintering between Ni particles. For compositions with larger vol % Ni (i.e. 55 vol % Ni), less YSZ is available to support the Ni and larger Ni particles would be expected. The resultant microstructures for the four compositions after 24 h of operation are shown in Figure 6. It is difficult to see any distinguishable difference for the three lowest Ni contents, 40, 45, and 50 %, although, the 55 % composition does show a dissimilarity. The Ni particles are larger and more easily distinguishable from the YSZ support.

Electrical conductivity measurements were also performed on all four compositions for 24 h, Figure 7. Since the samples contain various vol % Ni, a direct comparison cannot be made as to how the Ni particles are distributed within the cermet, although, similar trends were observed. All compositions had similar conductivities in the oxide form, ≈3-5 S/cm. Upon exposure to the fuel, a large increase in the conductivity occurred, within 5 min, then rapidly decreased within ≈3 h to a steady state value. The large increase in the conductivity is caused by the reduction of NiO to Ni metal. The very sharp decrease in conductivity is due to the rapid sintering between Ni particles, and the continued slow decrease in the conductivity can be attributed to further sintering of the Ni particles.

Effect of NiO Starting Raw Materials on Anodic Overpotentials

Three different NiO sources were used in this study to examine the effect of Ni particle size and preparation conditions on the anodic overpotential. All anodes contained 45 vol % Ni, and were fired onto the YSZ electrolyte at 1400°C. The first NiO powder was synthesized by the glycine nitrate process and calcined at 900°C as described previously. The remaining two sources were commercially available powders with different primary particle sizes. The first powder had a reported particle size of -325 mesh (< 45 μm) and the second powder was spray dried with a primary particle size less than 10 μm.

The η-j plots for the three different particle sizes initially and after 24 h are shown in Figure 8. The results of the powder prepared by the glycine nitrate process are the same as reported previously. The -325 mesh powder initially has an overpotential of ~ 250 mV at 600 mA/cm^2 but increases to ~ 370 mV after 24 h. The spray dried powder has a relatively stable overpotential but is extremely high, ~ 450 mV at 600 mA/cm^2. Examination of the microstructures after 24 h of operation revealed large, distinguishable Ni particles for both commercial powders. This can explain the large overpotentials in that the number of reaction sites (Ni-YSZ contacts) has drastically decreased due to the large Ni particle size. The microstructure of the spray dried powder resembles spray dried granules which eventually reduce to Ni spheres.

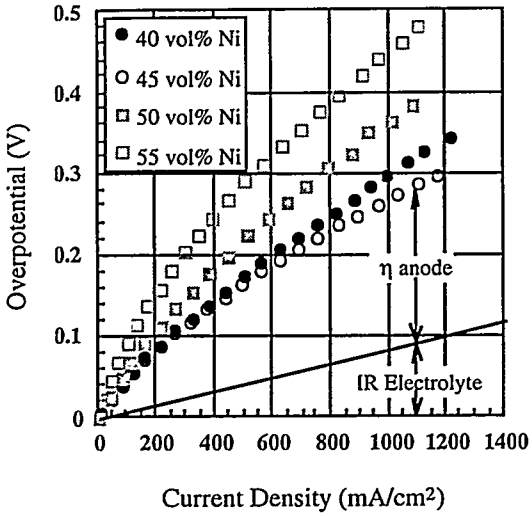

Figure 4. Initial η-j relations of Ni-YSZ cermets sintered at 1400°C.

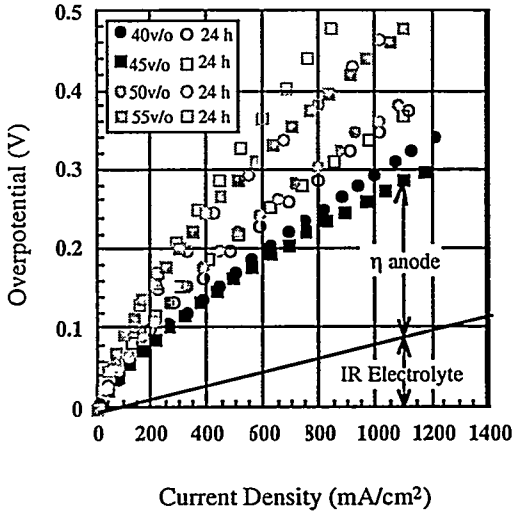

Figure 5. η-j results, initially and after 24 h, for Ni-YSZ cermets sintered at 1400°C.

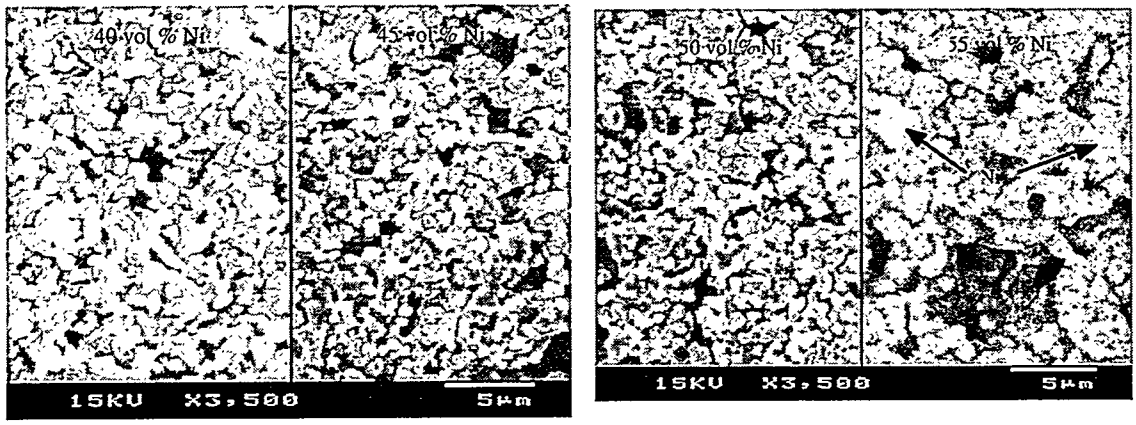

Figure 6. Microstructures of the 40, 45, 50 and 55 vol% Ni compositions.

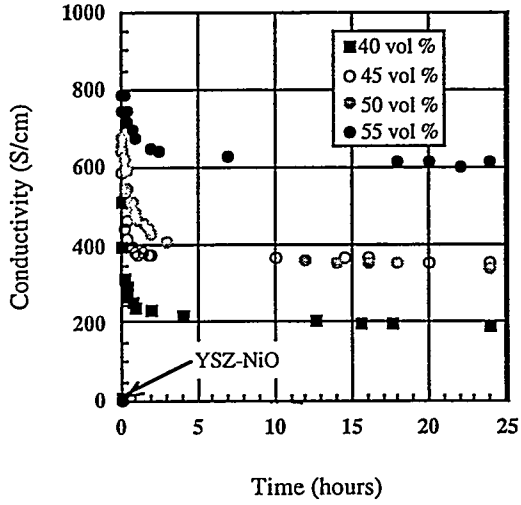

Figure 7. Variation in the σ with time for the Ni-YSZ cermets of figure 5.

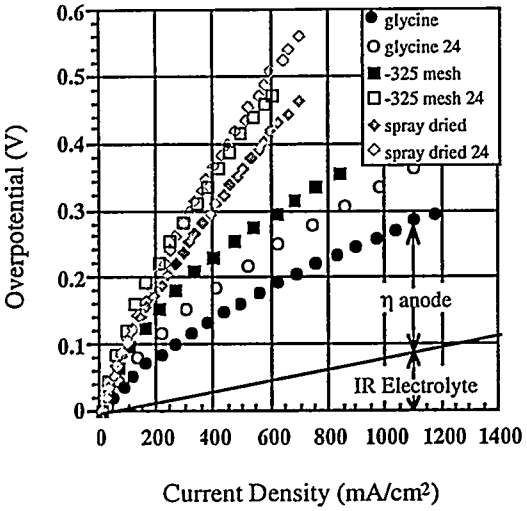

Figure 8. η-j relations of 45 vol % Ni compositions prepared with different NiO sources and sintered at 1400°C.

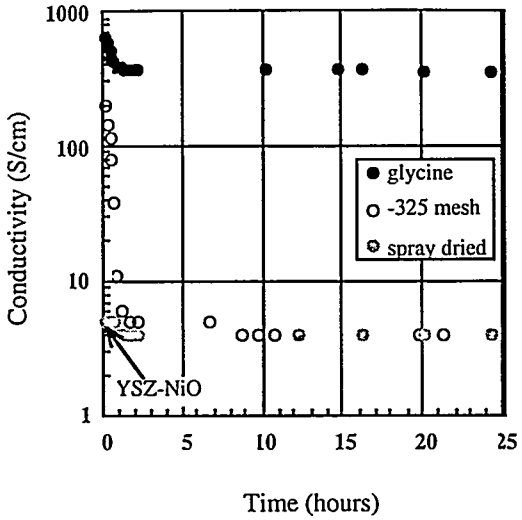

Figure 9. Conductivity versus time 45 vol % Ni compositions prepared with different NiO sources.

The conductivity for the three powders also correlates well with the electrochemical results (Figure 9). The conductivity of the spray dried powder was relatively stable upon reduction but was extremely low, comparable to the NiO-YSZ composite (≈3 S/cm). This suggests that the Ni particles have rapidly become large and separated from one another, decreasing the number of Ni-Ni contacts. The -325 mesh powder initially had a higher conductivity (≈200 S/cm) but quickly decreased to values comparable to the spray dried powder. This also suggest that the Ni particles have coarsened and reduced the number of Ni-Ni contacts throughout the cermet. For both commercial powders, the Ni-Ni and Ni-YSZ particle contacts has decreased causing the conductivity to be extremely low and the overpotential to be high.

Effect of Pre-calcination of Powders on Anodic Overpotentials

The influence of calcining NiO and YSZ together at high temperatures (1400°C) before depositing the composition onto the YSZ was investigated. This approach was examined to provide a more stable anode structure by allowing the YSZ and NiO powders to further densify during calcination. The composition studied was 50 vol % Ni; the η-j results are shown in Figure 10. For comparison, a 50 vol % Ni composition prepared by the conventional technique (described previously with no pre-calcination of NiO and YSZ) is also illustrated. Both the precalcined and conventionally prepared samples have the same starting raw materials, commercial YSZ and NiO prepared by the glycine nitrate process.

The pre-calcined powders resulted in a lower and more stable overpotential (≈240 mV at 1000 mA/cm^2) than the conventionally prepared composition (≈380 mV at 1000 mA/cm^2) after 24 h. The lower and more stable overpotential is believed to be caused by a more rigid and stronger YSZ structure due to the high temperature calcination of the YSZ and NiO. The pre-calcination treatment allows more densification to occur between YSZ particles because the anode is normally constrained to sinter by the YSZ electrolyte during annealing. Therefore, the pre-calcination treatment is more effective than the conventional preparation technique in preventing the Ni from coarsening during operation. The pre-calcined and conventionally prepared anode microstructures after 24 h of operation are shown in Figure 11. The precalcined anode resulted in larger grains (≈1-2 μm) and a coarser microstructure than the conventionally prepared anode due to the high temperature calcination treatment.

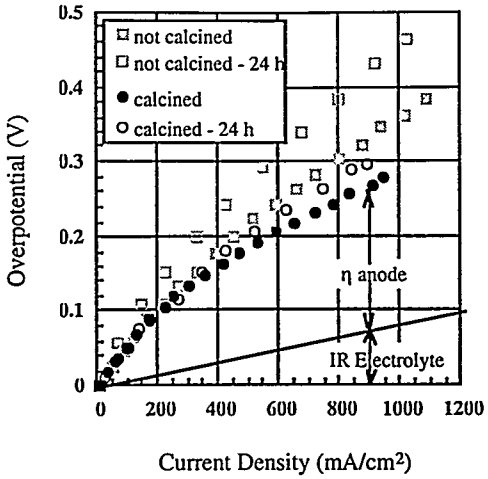

Figure 10. η-j relations of 50 vol % Ni compositions prepared by different techniques, NiO and YSZ calcined together at 1400°C, and by the conventional technique; all sintered at 1400°C.

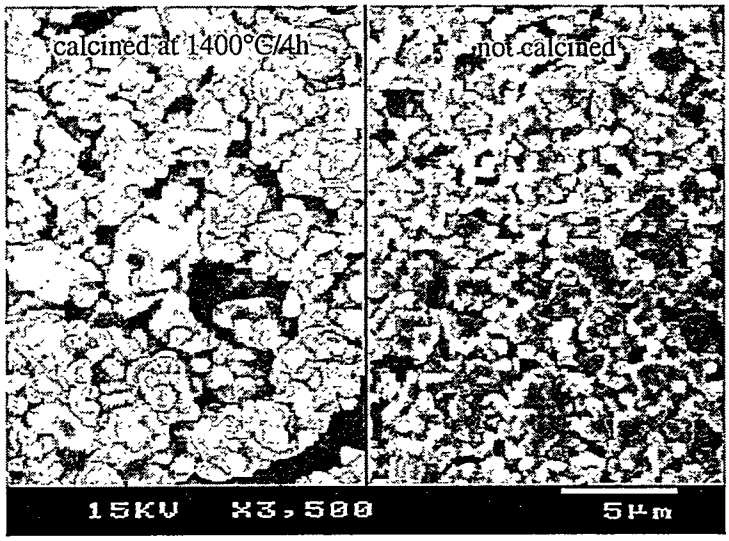

Figure 11. Microstructures of 50 vol % Ni compositions prepared by different techniques, NiO and YSZ calcined together at 1400°C and by the conventional technique; all sintered on the YSZ electrolyte at 1400°C.

4.2 Cathode Studies

Studies during 1997-98 indicated that excess Mn in the $LaMnO_3$ cathode would improve the performance. Further studies were performed and are presented here. Overpotential results are shown in figures 12 and 13 for 1, 5 and 10% excess Mn (also can be dubbed 1, 5 and 10% A-site deficient). While firing on the compositions at 1100°C did not appreciably change the properties, figure 13 clearly shows a large variation is observed for the compositions fired on at 1200°C. The 10 % excess Mn shows an extremely small overpotential (~ 40 mV at 1000 mA/cm^2). The 5% excess Mn composition also shows a lower overpotential (~ 80 mV at 1000 mA/cm^2) than the near stoichiometric sample (~ 105 mV at 1000 mA/cm^2). Because the grain sizes for the cathodes were observed to be very similar, this cannot be used as the basis for the large variation in the

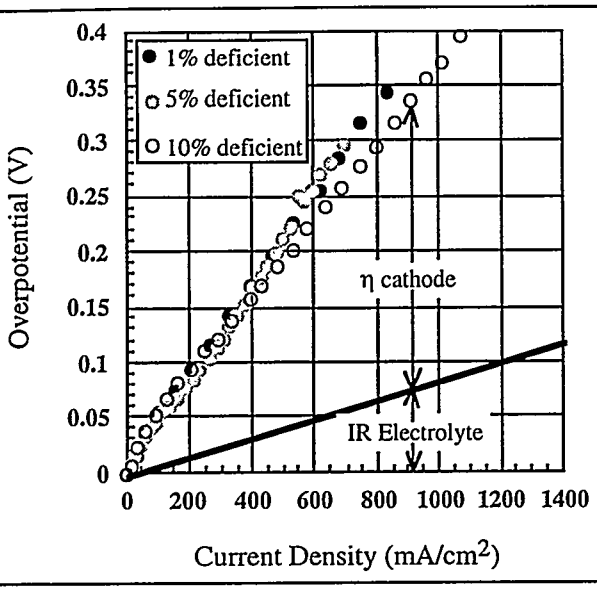

Figure 12. η-j relations of the three Sr doped $LaMnO_3$ compositions calcined at 900°C and sintered at 1100°C.

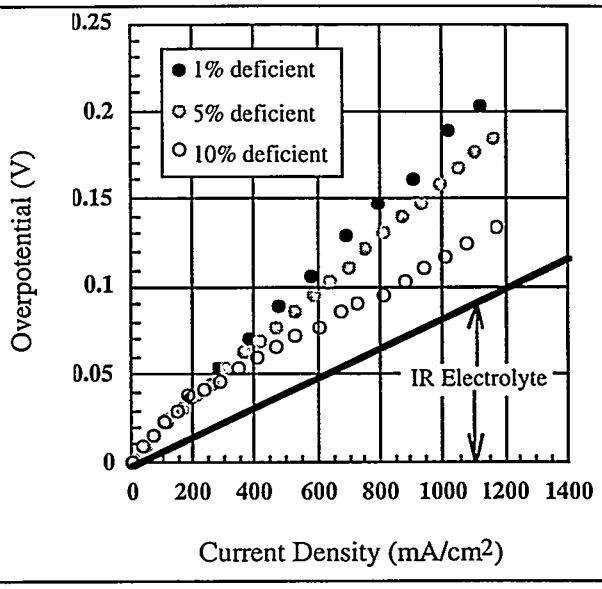

Figure 13. η-j relations of the three Sr doped $LaMnO_3$ compositions calcined at 900°C and sintered at 1200°C.

electrochemical behavior. X-ray diffraction was performed to see if a second phase (i.e. $La_2Zr_2O_7$) could be detected at the interface. Bilayer structures (LSM/YSZ) were fabricated in a similar manner as described for DC conductivity experiments with thinner cathodes (~ 7-8 μm). The cathode face was exposed to the X-ray beam to examine the LSM/YSZ interface. The XRD patterns for the three compositions annealed at 1200°C showed the same diffraction peaks corresponding to the YSZ and LSM phases except for the $La_{0.79}Sr_{0.2}MnO_3$ sample which had an extra peak at ~28.5°, corresponding to the 100 % intensity line of the $La_2Zr_2O_7$ phase. Therefore, the addition of excess Mn is effective in decreasing the pyrochlore phase formation at the interface at higher temperatures (≤ 1200°C). Quantitatively, nothing can be said about the pyrochlore phase except that the stoichiometric composition shows a greater amount of $La_2Zr_2O_7$ formed at the interface than the Mn excess compositions. The Mn excess compositions may also have the pyrochlore phase at the interface but may be small enough (i.e. thickness ~ Å or nm level) that it is not detected by the diffractometer. It would be predicted that the 5 % excess Mn composition should form the $La_2Zr_2O_7$ phase at the interface as a function of temperature and time before the 10 % composition. This would help explain the higher overpotentials. Another possible explanation for the difference in the electrochemical behavior for the 5 and 10% Mn excess sample (assuming no pyrochlore has formed at the interface) is that equilibrium has yet to be attained after 24 h.

Figure 14 is the η-j plot of the three compositions fired at 1300°C. A similar type of trend is observed as was for the 1200°C firing except that the overpotentials have increased. The resultant overpotentials for $La_{0.70}Sr_{0.2}MnO_3$, $La_{0.75}Sr_{0.2}MnO_3$, and $La_{0.79}Sr_{0.2}MnO_3$, at 1000 mA/cm^2 are ~ 90, 100, and 130 mV. The increase in the measured overpotentials compared to the lower sintering temperature (1200°C) can be attributed to both an increase in the grain size (less TPBs) and a greater amount of $La_2Zr_2O_7$ formed at the interface. It is assumed that more Mn would diffuse into the YSZ, resulting in a thicker interfacial reaction product, as the temperature and time of exposure were increased.

The overpotential results for the three compositions fired at 1400°C are shown in Figure 15. The 1 % and 10 % excess Mn compositions show a consistent trend with the lower sintering temperatures, namely, that the overpotentials are larger due to both a larger grain size and an increased reaction at the interface. The overpotential values for the 1 and 10 % excess samples at 1000 mA/cm^2 are ~ 210 and 100 mV. The 5 % excess sample has a very high overpotential (~ 320 mV at 1000mA/cm^2), and is not consistent with the previously observed trends. Some possible explanations could be that the sample was cracked or improperly sealed which allowed the mixing

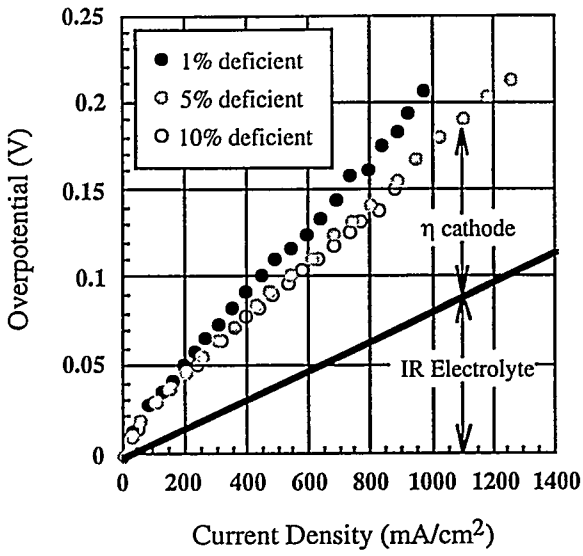

Figure 14. η-j relations of the three Sr doped $LaMnO_3$ compositions calcined at 900°C and sintered at 1300°C.

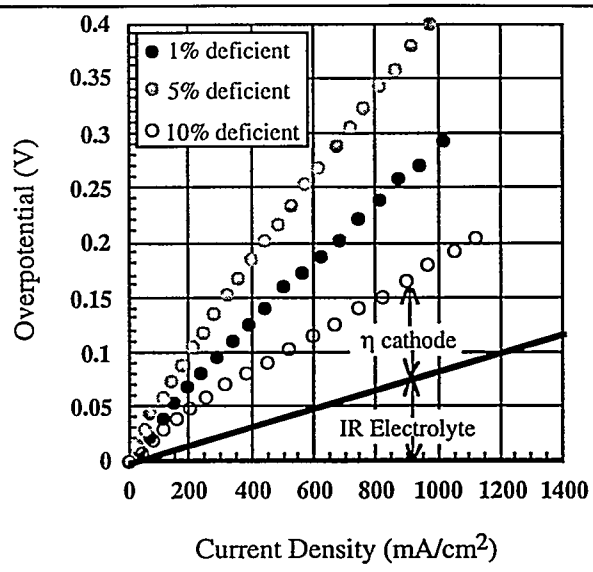

Figure 15. η-j relations of the three Sr doped $LaMnO_3$ compositions calcined at 900°C and sintered at 1400°C.

of the fuel and oxidant which could reduce the oxygen pressure in the cathode chamber. Another possible explanation is that the sample has not equilibrated within the 24 h period.

The three compositions were also sintered onto a YSZ substrate at 1450°C to see if a second phase could be detected using the SEM. The resultant microstructures of the YSZ/LSM interfaces are shown in Figure 16. No second phase at the interface was observed, therefore, X-ray diffraction was used to analyze the bilayers as described previously. All three composition show the pyrochlore phase development at the interface. Again, nothing quantitative will be said about the amount of $La_2Zr_2O_7$ formed at the interface.

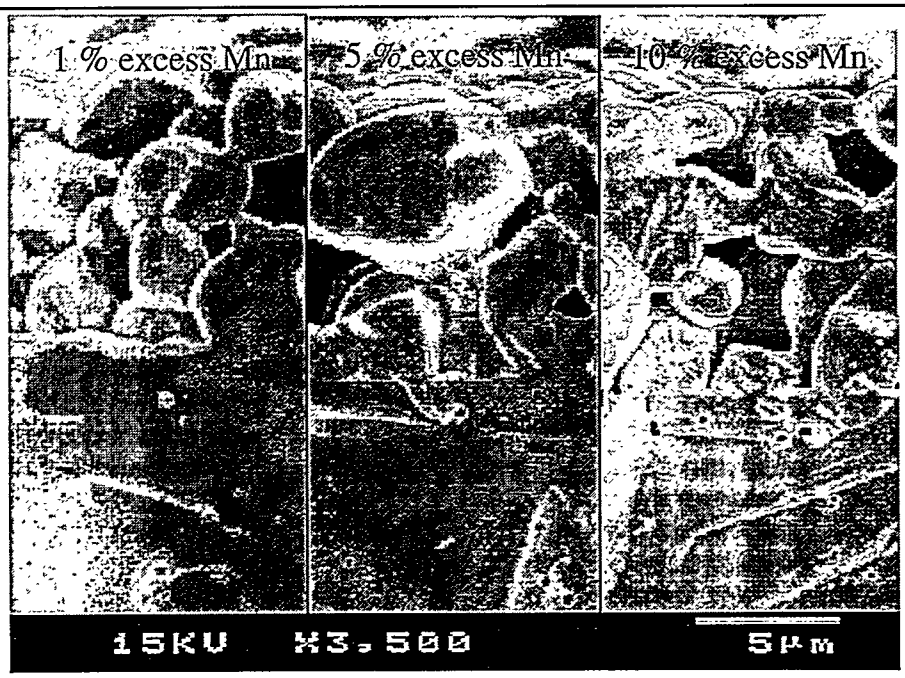

Figure 16. Microstructures of $La_{0.79}Sr_{0.20}MnO_3$, $La_{0.75}Sr_{0.20}MnO_3$, and $La_{0.70}Sr_{0.20}MnO_3$ sintered on the YSZ electrolyte at 1450°C for 24 h.

4.3 Thin Film Studies

In previous studies at UMR 100% dense films of a large number of binary, ternary, and quaternary oxides have been fabricated which are important to the electrical ceramics community *(U.S. Patent # 5,494,700. H.U. Anderson, C.C. Chen and M.M. Nasrallah, "Method of Coating A Substrate with a Metal Oxide Film From and Aqueous Solution Comprising a Metal Cation and a Polymerizable Organic Solvent," February 1996).* Of interest for the SOFC community are thin films based on $SrCeO_3$, CeO_2, ZrO_2, $LaMnO_3$, $(La,Sr)(Fe,Co)O_3$, and $LaGaO_3$. A variety of dense substrates such as silicon, metals, alumina, zirconia and glass have been used to support these films. These films are simply produced through chelation of the appropriate cations into a polymer precursor; when deposited on a substrate the polymer dries to form a continuous film. Typically these films form either amorphous or crystalline oxides when heated to ≈300°C. This technique allows mixing of the cations on the molecular level, hence it is very useful for the preparation of homogenous, multicomponent oxide films. The majority of studies have used spin coating at the application process, but by controlling the solution viscosity and the cation concentration, a variety of other deposition techniques can be used such as dip coating, doctor-blading, and spraying. Results obtained on films of ZrO_2 based films are of particular interest in that nanocrystalline YSZ (g.s. ≤ 100 nm) shows a greatly enhanced σ_i of ≈ 0.1 S/cm at 600°C (figure 17). This is a value ≈30 times that of 1000 nm YSZ.

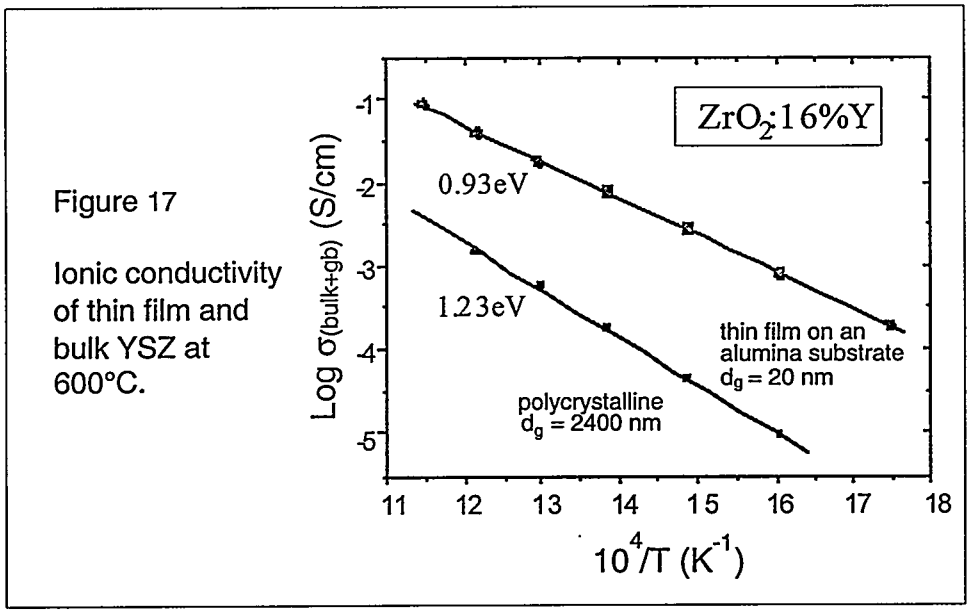

Figure 17

Ionic conductivity of thin film and bulk YSZ at 600°C.

This suggests that if SOFC's can be produced with an electrolyte with a g.s. ≤ 100 nm, then the overall electrolyte resistance can be reduced to a negligible level. Our studies have shown that the grain size is not dependent upon the film thickness, but is dependent upon the annealing temperature of the film (figure 18). In addition, the grain size of films annealed at 900°C remains about 20 nm irrespective of the film thickness (5 to 1000 nm). This suggests that if such films can be produced on a porous cathode, then microstructure-stable SOFC's based on such thin films can be operated at temperatures below 700°C.

Marked success has been achieved on the placement of thin YSZ electrolytes on porous Ni/YSZ electrodes. The process being used is a "transfer technique" in which dense YSZ films are initially fabricated on NaCl substrates, followed by partial dissolution of the substrate and placement of the film on the porous substrate. Heating the substrate to 400°C results in a firmly attached films (figure 19); higher temperatures result in grain growth. This technique has allowed us to produce structures with film thicknesses ranging from 70 to 3000 nm, and grain sizes ranging from 2 to 300 nm. I-V measurements of single cells produced by this technique have been initiated within the last month. Early results are very encouraging and indicate that we indeed can

Figure 18

Variation in grain size with sintering temperature for YSZ thin films deposited on polycrystalline and single crystal alumina.

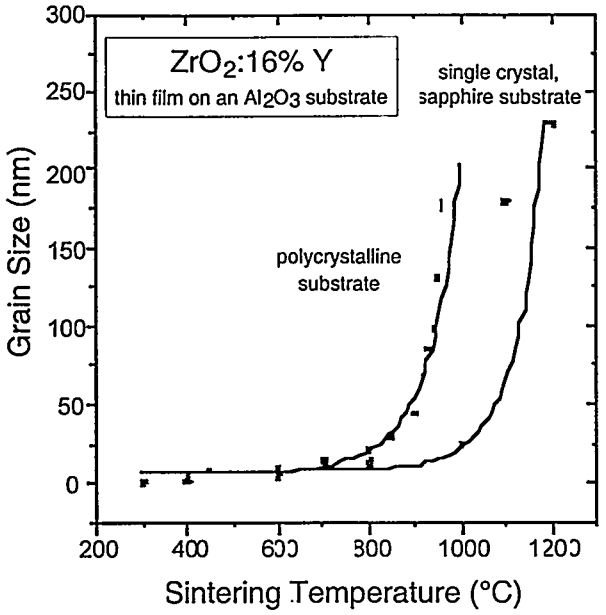

Figure 19

YSZ thin film fired on a YSZ:Ni porous anode at 400°C.

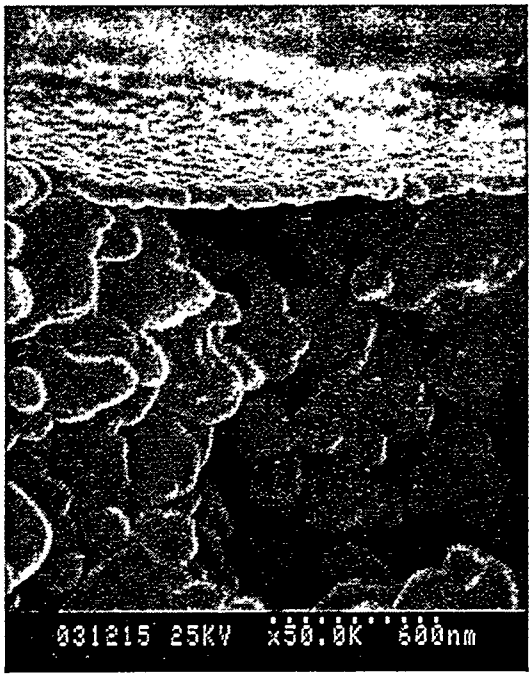

produce dense, nonporous YSZ electrolytes at temperatures in the 400 to 700°C range. These results are currently serving as a vehicle in which the influence of microstructure and electrolyte thickness on cell performance can be evaluated.

5.0 CONCLUSIONS

In this research the microstructure ↔ property relations in solid oxide fuel cells (SOFC's) are being studied to better understand the mechanisms involved in cell performance. The overall aim is to fabricate SOFC's with controlled, stable, high performance microstructures. Most cathode studies were completed in the last DOE contract; studies during this year focused more on the influence of nonstoichiometry on the electrical performance. Studies indicate that nonstoichiometric $La_xSr_{0.20}MnO_3$(x=0.70, 0.75, and 0.79) cathode compositions exhibit the best properties. A series of studies using these compositions fired on at temperatures of 1100, 1200, 1300 and 1400°C were performed. In all instances, 1200°C was the optimum, with the x=0.70 composition being the best. It has an overpotential of only 0.04V at 1 A/cm^2. SEM analyses indicated no second phases or interdiffusion is detectable.

Studies on optimization of anode compositions yielded the optimum volume fraction of Ni (45vol%), the best sintering temperature / time (1400°C/2 h), and the best starting materials (glycine-nitrate derived NiO and "normal" YSZ). In essence these results simply reflect the optimum microstructure. As such, they are being used to guide the development of optimized anodes for lower temperature operation based on Cu/CeO_2 cermets.

Marked success has been achieved on the placement of thin YSZ electrolytes on porous Ni/YSZ electrodes. The process being used is a "transfer technique" in which dense YSZ films are initially fabricated on NaCl or polymeric substrates, followed by partial dissolution of the substrate and placement of the film on the porous substrate. This technique has allowed us to produce structures with film thicknesses ranging from 70 to 3000 nm, and grain sizes ranging from 2 to 300 nm. Cells based on electrolytes this thick should operate in the 400 – 700°